Technical Description of Advanced LIGO Detector by Subsystem

Fred Raab
LIGO-T1800389

Condensed from the article published as Class. Quantum Grav. 32 (2015) 074001, also publicly available as https://arxiv.org/abs/1411.4547. The published article gives many of the scientific reasons for technical choices, which are not included in this technical description.

1. Interferometer configuration and system design

The optical configuration of the Advanced LIGO interferometer is shown in Figure 1. The basis of the design is a Michelson interferometer with a Fabry-Perot resonant cavity in each arm. The power recycling mirror (PRM) forms a resonant cavity between the laser source and the Michelson to increase the effective laser power. The signal recycling mirror (SRM) at the anti-symmetric output of the Michelson is used to effectively lower the arm cavity finesse for gravitational wave signals and thereby maintain a broad detector frequency response.

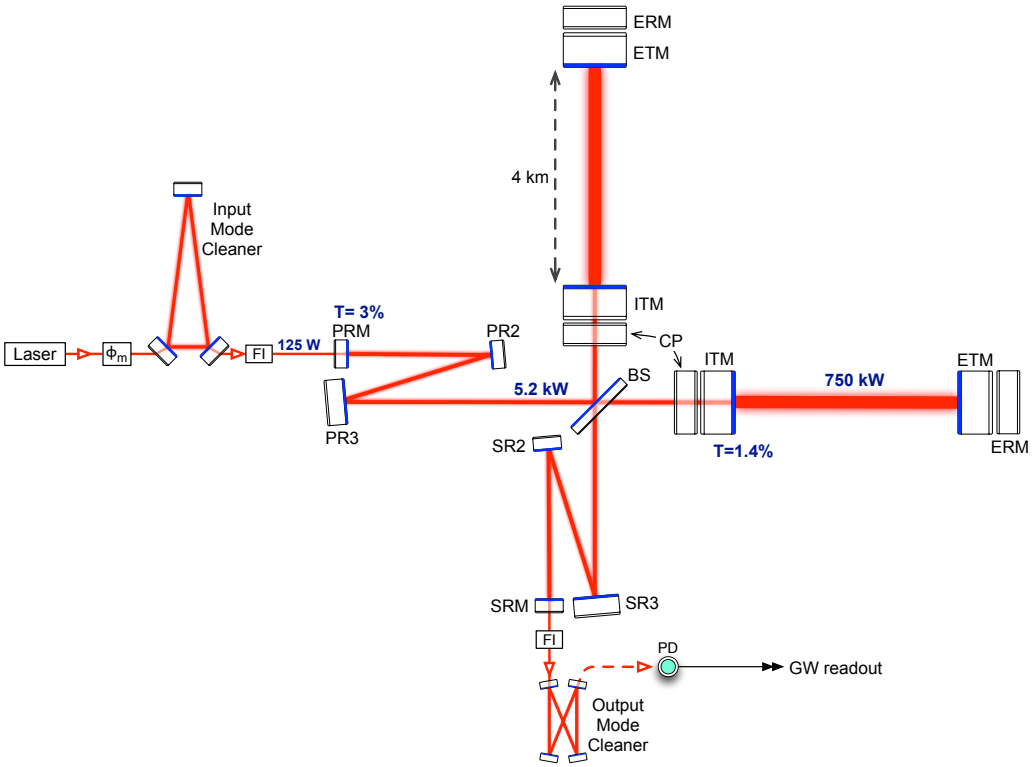

Figure 1. Advanced LIGO optical configuration. ITM: input test mass; ETM: end test mass; ERM: end reaction mass; CP: compensation plate; PRM: power recycling mirror; PR2/PR3: power recycling mirror 2/3; BS: 50/50 beam splitter; SRM: signal recycling mirror; SR2/SR3: signal recycling mirror 2/3; FI: Faraday isolator; φ_m: phase modulator; PD: photodetector. The laser power numbers correspond to full-power operation. All of the components shown, except the laser and phase modulator, are mounted in the LIGO ultra-high vacuum system on seismically isolated platforms.

The top-level parameters of the interferometers are listed in Table 1. The various interferometer subsystems and components are described in section 2.

Table 1. Main parameters of the Advanced LIGO interferometers. PRC: power recycling cavity; SRC: signal recycling cavity.

Parameter	Value
Arm cavity length	3994.5 m
Arm cavity finesse	450
Laser type and wavelength	Nd:YAG, λ = 1064 nm
Input power, at PRM	up to 125 W
Beam polarization	linear, horizontal
Test mass material	Fused silica
Test mass size & mass	34cm diam. x 20cm, 40 kg
Beam radius ($1/e^2$), ITM / ETM	5.3 cm / 6.2 cm
Radius of curvature, ITM / ETM	1934 m / 2245 m
Input mode cleaner length & finesse	32.9 m (round trip), 500
Recycling cavity lengths, PRC / SRC	57.6 m / 56.0 m

2. Detector subsystems

2.1 Laser source

The interferometer employs a multi-stage Nd:YAG laser that can supply up to 180 W at the laser system output. The pre-stabilized laser (PSL) system consists of this laser light source, and control systems that stabilize the laser in frequency, beam direction, and intensity. The laser was developed and supplied by the Max Planck Albert Einstein Institute in collaboration with Laser Zentrum Hannover e.V. A schematic drawing of the PSL is shown in Figure 2.

The laser comprises three stages. The first stage is a commercial non-planar ring-oscillator (NPRO) manufactured by InnoLight GmbH. The second stage (medium power amplifier) is a single-pass amplifier that boosts the NPRO power to 35 W, and the third stage is an injection-locked ring oscillator with a maximum output power of about 220 W. All stages are pumped by laser diodes; the pump diodes for the second and third stages are fibre coupled and located far from the laser table for easier management of power and cooling. The system may be configured for 35 W output by using the NPRO and medium power stages, bypassing the high power oscillator; this configuration will be in the early operations of Advanced LIGO.

The source laser is passed through the pre-mode cleaner (PMC). The PMC is a bow-tie cavity (2m round trip length) designed to strip higher-order modes from the beam, to reduce beam jitter (amplitude reduction factor for TEM_{01}/TEM_{10} modes of 63), and to provide low-pass filtering for RF intensity fluctuations (cavity pole at 560 kHz).

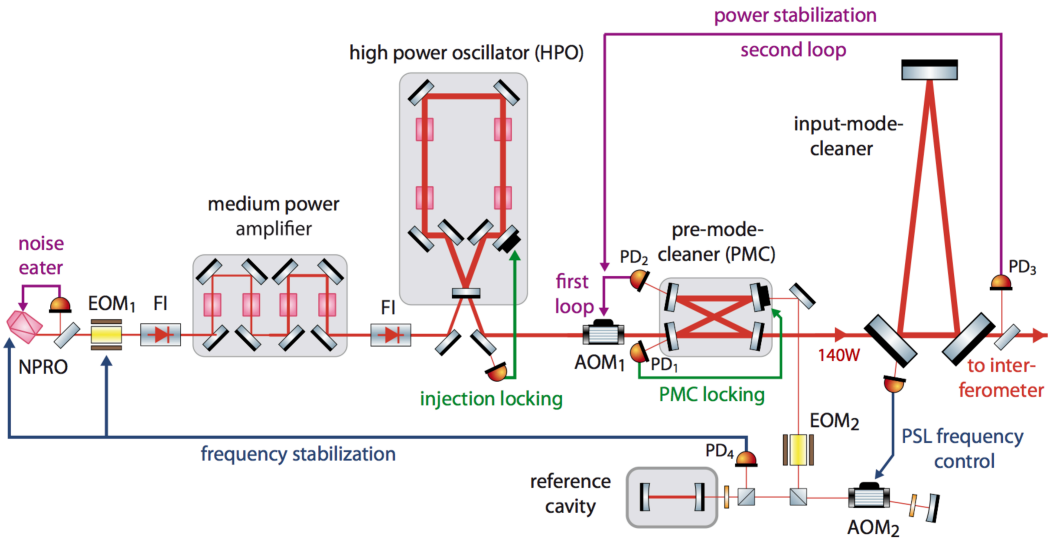

Figure 2 Schematic of the pre-stabilized laser system. The Input Mode Cleaner is discussed in section 4.2. AOM: acousto-optic modulator; EOM: electro-optic modulator; FI: Faraday isolator; PD: photodetector.

The residual intensity noise specification is 2×10^{-9} $Hz^{-1/2}$ at 10 Hz, at the input to the PRM.

The initial frequency stabilization of the laser is performed in the PSL by locking its frequency to an isolated, high-finesse reference cavity (bandwidth of 77 kHz) using the standard reflection locking technique. Three actuators are used to provide wide bandwidth and large dynamic range: a PZT attached to the NPRO crystal; an electro-optic modulator (EOM_1)—used as a broadband, phase corrector—between the NPRO and medium power amplifier; and the NPRO crystal temperature for slow, wide-range control. The servo bandwidth is 400 kHz. The beam used for this frequency pre-stabilization is taken after the PMC, and is double-passed through an AOM before being sent to the reference cavity. This AOM is driven by a voltage-controlled oscillator to provide laser frequency actuation (1 MHz range, 100 kHz bandwidth) for subsequent stages of stabilization.

2.2 Input optics

The input optics subsystem (IO) accepts the light from the pre-stabilized laser, stabilizes and conditions it, and performs matching and pointing into the main interferometer core optics. A schematic view is shown in Figure 3. The optical efficiency of the IO, from the PSL output to the PRM, is designed to be at least 75%. The system can be broken down into the following functional units.

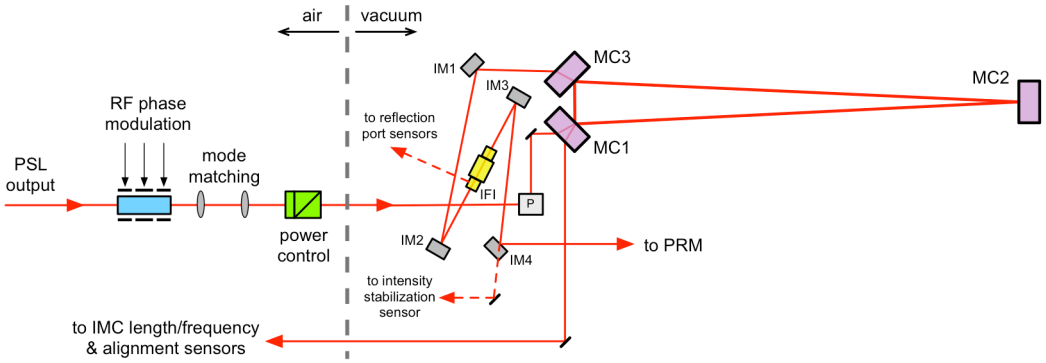

Figure 3 Schematic of the input optics components. IFI: input Faraday isolator. P: periscope. IMn: input mirror 1-4.

2.2.1 RF Modulation. Radio-frequency (RF) phase modulation is impressed on the beam and used for global sensing of the interferometer (see section 2.8) and for sensing of the IMC. Three modulation frequencies are applied, all with small modulation depth: 9 MHz and 45 MHz for the main interferometer sensing; 24 MHz for IMC sensing. The EOM uses a 40mm long, 4×4 mm cross-section, wedged RTP (rubidium titanyl phosphate) crystal as the electro-optic material. Three pairs of electrodes are used to apply the three modulation frequencies to the crystal.

2.2.2 Input Mode Cleaner. The IMC supplies a key function of the IO system: to stabilize the PSL beam in position and mode content, and to provide a high-quality laser frequency reference. The beam pointing stability at the input to the PRM, expressed relative to the beam radius and beam divergence angle, must be $<1\text{x}10^{-8}$ $\text{Hz}^{-1/2}$ at 100 Hz. The frequency stability at the IMC output must be $<1\text{x}10^{-3}$ $\text{Hz/Hz}^{1/2}$ at 100 Hz.

The IMC is a three-mirror ring cavity used in transmission. Each mirror is suspended in a triple pendulum suspension with metal wire loops (see section 4.4) to provide vibration isolation and acceptable thermal noise. The IMC finesse is 500, the round trip length is 32.9 m, and the linewidth is 18 kHz. The 24 MHz phase modulation sidebands are used both for reflection locking and wavefront-sensor alignment control of the IMC. Additionally, the IMC is used as a frequency actuator for the final level of frequency stabilization to the long arm cavities.

2.2.3 Faraday Isolator. An in-vacuum Faraday Isolator is mounted between the IMC output and the PRM; the isolator extracts the beam reflected from the interferometer and prevents this beam from creating parasitic interference in the input chain. The isolator must deliver a minimum of 30dB of isolation up to 125 W of laser power. To compensate thermally induced birefringence, the isolator uses two terbium gallium garnet (TGG) crystals for Faraday rotation, with a quartz rotator in between. Compensation of thermal lensing is achieved by incorporating a negative *dn/dT* material (deuterated potassium dihydrogen phosphate, or 'DKDP') in the assembly[1].

2.2.4 Mode Matching. The IMC output beam must be matched to the interferometer mode, with a targeted efficiency of 95% or better. This mode matching is accomplished with two curved mirrors, in combination with two flat mirrors used for beam routing. All four of these reflective optics are mounted in single stage suspensions for vibration isolation; the suspensions also have actuators to provide remote steering capability (see section 2.4).

2.3 Core optics

The 'Core Optics' are central to the interferometer performance. For each interferometer they include (see Table 2):

- Two input and two end test masses which form the Fabry-Perot arms
- A 50/50 beamsplitter at the vertex of the Michelson interferometer
- Two compensation plates that serve as actuation reaction masses for the input test masses, and to which thermal compensation can be applied
- Two actuation reaction masses for the end test masses
- Four reflective curved mirrors in the signal and power recycling cavities
- Signal and power recycling mirrors

Table 2 Parameters of the core optics. ETM/ITM: end/input test mass; CP: compensation plate; ERM: end reaction mass; BS: beam splitter; PR3/2: power recycling mirror 3/2; SR3/2: signal recycling mirror 3/2; PRM/SRM: power/signal recycling mirror. ROC: radius of curvature; AR: anti-reflection. Transmission values are at 1064 nm, except for those in parentheses, which are for 532 nm.

Optic	Dimensions: diam. × thickness	Mass	Transmission	ROC	Beam size ($1/e^2$ radius)
ITM	34 × 20 cm	40 kg	1.4% (0.5-2%)	1934 m	5.3 cm
ETM	34 × 20 cm	40 kg	5 ppm (1-4%)	2245 m	6.2 cm
CP	34 × 10 cm	20 kg	AR< 50 ppm	flat	5.3 cm
ERM	34 × 13 cm	26 kg	AR< 1000 ppm	flat	6.2 cm
BS	37 × 6 cm	14 kg	50%	flat	5.3 cm
PR3	26.5 × 10 cm	12 kg	< 15 ppm	36.0 m	5.4 cm
SR3	26.5 × 10 cm	12 kg	< 15 ppm	36.0 m	5.4 cm
PR2	15 × 7.5 cm	2.9 kg	225 ppm (>90%)	-4.56 m	6.2 mm
SR2	15 × 7.5 cm	2.9 kg	< 15 ppm	-6.43 m	8.2 mm
PRM	15 × 7.5 cm	2.9 kg	3.0%	-11.0 m	2.2 mm
SRM	15 × 7.5 cm	2.9 kg	20%	-5.69 m	2.1 mm

All the core optics are made with fused silica substrates. The fused silica material used for the input test masses, the compensation plates, and the beamsplitter is Heraeus Suprasil 3001. This is an ultra-low absorption grade, with absorption at 1064 nm of < 0.2 ppm/cm. The material also has a low level of inhomogeneity and low mechanical loss. The material for the other core optics is less critical, and less expensive grades of fused silica are used (ETMs use Heraeus Suprasil 312).

Table 3 lists the test mass substrate polishing requirements, as well as typical achieved levels. The substrates for the large core optics are produced by a combination of super-polishing for small scale smoothness, followed by ion-beam milling to achieve the large scale uniformity. Coating material parameters are given in Table 4.

Table 3 Polishing specifications and results for the test masses

	Surface error, central 160 mm diam., power & astigmatism removed, rms		**Radius of curvature spread**
	> 1 mm^{-1}	**1—750 mm^{-1}**	
Specification	< 0.3 nm	< 0.16 nm	-5, +10 m
Actual	0.08—0.23 nm	0.07—0.14 nm	-1.5, +1 m

Table 4 Test mass coating material parameters used to calculate coating thermal noise (i.e., this represents our model of the coating).

Parameter	**Low-index: silica**	**High-index: tantala**
Mechanical loss	4×10^{-5}	2.3×10^{-4}
Index of refraction	1.45	2.0654
dn/dT	8×10^{-6} / K	1.4×10^{-5} / K
Thermal expansion coefficient	5.1×10^{-7} / K	3.6×10^{-6} / K
Young's modulus	72 GPa	140 GPa
Layer optical thickness, ITM / ETM	0.308 λ / 0.27 λ	0.192 λ / 0.23 λ

All core optics are characterized with high precision metrology, before and after coating. Comparing the phase map residuals over the central 160 mm diameter, after subtracting tilt and power, gives:

- **ETM** substrate: 0.18 nm-rms coated: 0.69 nm-rms
- **ITM** substrate: 0.15 nm-rms coated: 0.31 nm-rms.
- Absorption in the test mass high-reflectivity coatings is specified at less than 0.5 ppm, and actual coatings show measured absorption of 0.2—0.4 ppm. Other coatings are specified to have absorption less than 1 ppm.

2.4 Suspensions

All of the primary in-vacuum interferometer optical components (all depicted in Figure 1, with the exception of the input Faraday isolator) are suspended by pendulum systems of varying designs. These suspension systems provide passive isolation from motion of the seismically isolated optics tables in all degrees of freedom and acceptable thermal noise. The suspensions also provide low noise actuation capability, used to align and position the optics based on interferometer sensing and control signals.

2.4.1 Requirements. The suspension designs employed for each optical element depend upon the performance requirements and physical constraints, as listed in Table 5. Most of the suspensions employ multiple pendulum and vertical isolation stages.

Table 5 Suspension types. Auxiliary suspensions are for optical pick-off beams, beam steering and mode matching.

Optical Component	vertical isolation stages	pendulum stages	Final stage fiber type	Longitudinal noise requirement @ 10 Hz (m/√Hz)
Test Masses (ITM, ETM)	3	4	Fused silica	1×10^{-19}
Beamsplitter (BS)	2	3	Steel wire	6×10^{-18}
Recycling cavity optics	2	3	Steel wire	1×10^{-17}
Input Mode Cleaner (IMC) optics	2	3	Steel wire	3×10^{-15}
Output Mode Cleaner (OMC) Assy	2	2	Steel wire	1×10^{-13}
ETM Transmission Monitor	2	2	Steel wire	2×10^{-12}
Auxiliary suspensions	1	1	Steel wire	2×10^{-11}

2.4.2 Design description. The most challenging design is the quadruple pendulum suspension for the test masses[2]. This is shown in Figure 4. Each of these suspensions is comprised of two adjacent chains, each chain having four masses suspended from one another. The main chain includes the test mass optic as the lowest mass. The adjacent, reaction chain provides an isolated set of masses for force reaction. The bottom mass in the reaction chain is the Compensation Plate (CP) optic in the case of an ITM suspension, and the End Reaction Mass (ERM) in the case of an ETM suspension. A structure surrounds and cages the suspended masses and mounts to the seismically isolated optics table.

Vibration isolation for the test mass is accomplished with a 4-stage pendulum and 3 stages of cantilevered blade springs, providing isolation in all 6 degrees-of-freedom above approximately 1 Hz. The suspension is designed to couple 22 of the 24 quasi-rigid body modes (all but the 2 highest frequency) of each isolation chain so that they are observable and controllable at the top mass (4 wires between masses to couple pitch and roll modes; non-vertical wires to couple pendulum modes). The blade springs are made of maraging steel to minimize noise resulting from discrete dislocation movements associated with creep under load[3].

For each chain, all the quadruple suspension rigid body modes below 9 Hz can be actively damped from the top stage. Sensing for this local damping is accomplished with integral optical shadow sensors[4], or with independent optical lever sensors. The shadow sensors are collocated with the suspension actuators and have a noise level of 3×10^{-10} m/√Hz at 1 Hz.

Force actuation on the upper three masses is accomplished with coil/magnet actuators[4]. Six degree-of-freedom actuation is provided at the top mass of each chain, by reacting against the suspension structure. These actuators are used for the local damping of 22 modes (each chain). The next two masses can be actuated in the pitch, yaw and piston

directions, by applying forces between adjacent suspended masses. These stages are used for global interferometer control. Low noise current drive electronics, combined with the passive filtering of the suspension, limit the effect of actuation noise at the test mass.

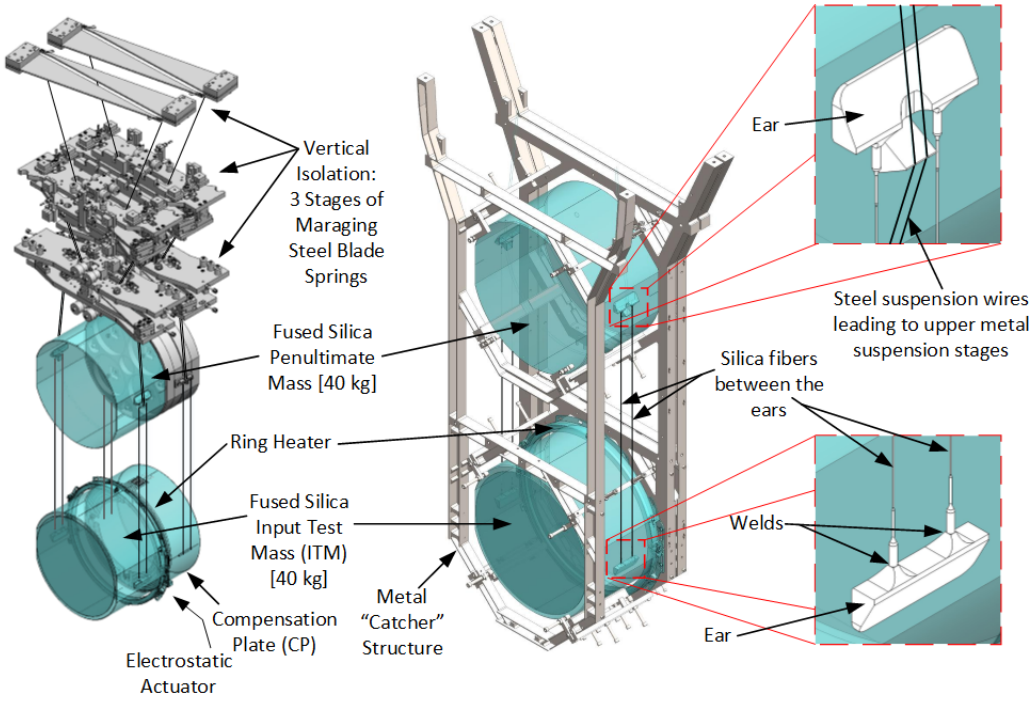

Figure 4 Quadruple pendulum suspension for the Input Test Mass (ITM) optic.

Direct low-noise, high-bandwidth actuation on the test mass optic is accomplished with electro-static actuation[5]. The CP and ERM each have an annular pattern of gold electrodes, deposited on the face adjacent to the test mass, just outside the central optical aperture. The pattern is separated into 4 quadrants, which enables actuation in pitch, yaw and piston.

The test mass and the penultimate mass are a monolithic fused silica assembly, designed to minimize thermal noise. Machined fused silica elements ("ears") are hydroxide-catalysis (silicate) bonded to flats polished onto the sides of the TM and penultimate mass. Custom drawn fused silica fibres are annealed and welded to the fused silica ears with a CO_2 laser system[6]. The shape of the fibres is designed to minimize thermal noise (400 µm dia. by 596 mm long with 800 µm dia. by 20 mm long ends).

The other suspension types employ the same basic key principles as the test mass quadruple suspensions, except for using steel wire in the final stage.

2.5 Seismic isolation

The general arrangement of the seismic isolation system and its relationship to the vacuum system and the suspension systems is illustrated in Figure 5, where a cut-away view of one of the test mass vacuum chambers is also shown.

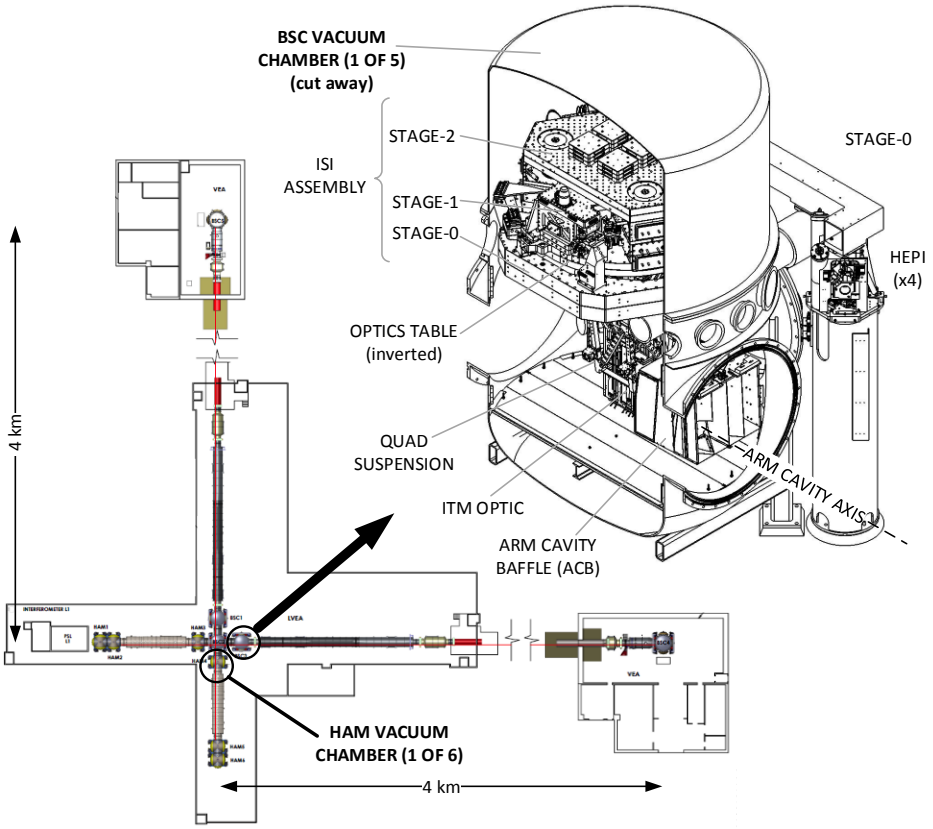

Figure 5 An Input Test Mass (ITM) vacuum chamber.

2.5.1 Requirements. The motion of the detector components, especially the interferometer optics, must be limited to very small amplitudes. The conceptual approach for seismic isolation is to provide multiple stages of isolation, as depicted in Figure 6. The stages topologically closest to the ground are referred to as the seismic isolation system; they provide coarse alignment, and employ both active and passive isolation to deal with the highest amplitude of motion. An optics table provides the interface between the seismic isolation system and the subsequent suspension system. The optics tables in the smaller (HAM) vacuum chambers are 1.9 m by 1.7 m; the downward-facing optics tables in the larger (BSC) vacuum chambers are 1.9 m diameter. The limits to optics table motion (Table 6) are derived from the allowed motion for the interferometer optics using the passive isolation performance of the suspension systems.

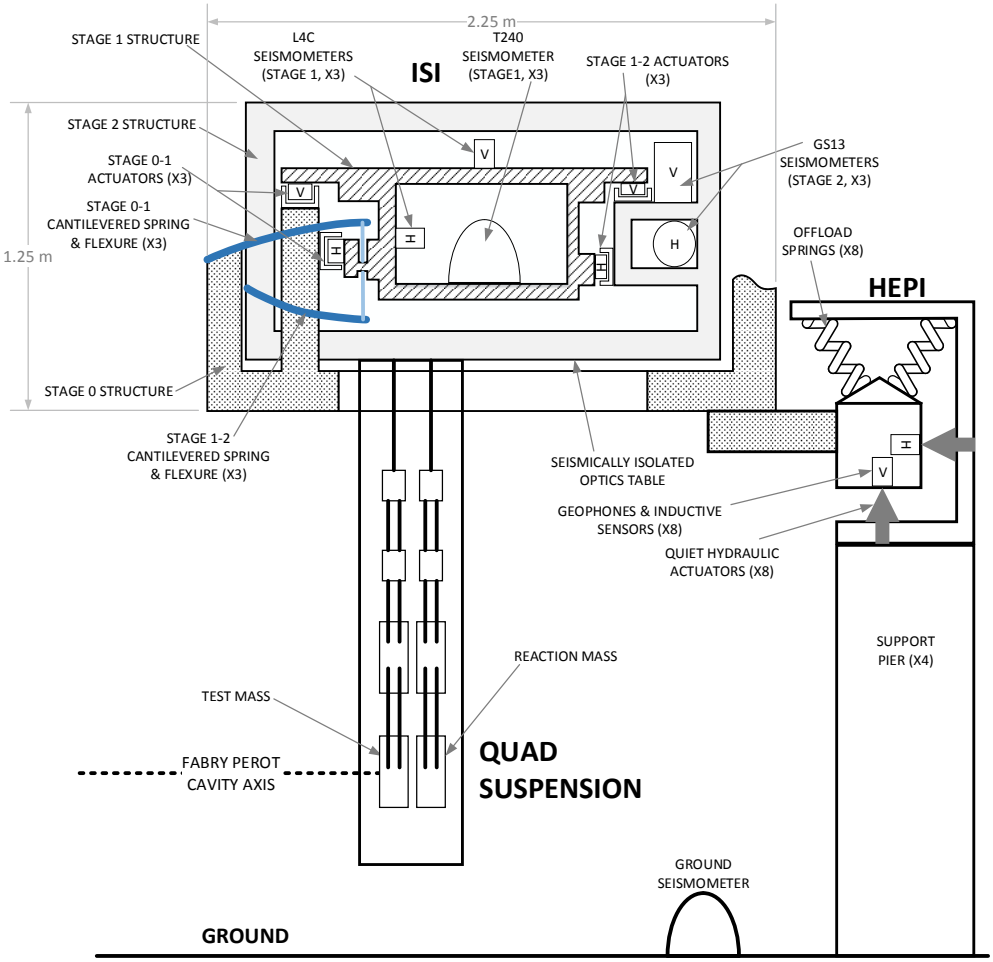

Figure 6 Seismic isolation for the test mass optic.

Table 6 Seismic isolation performance requirements for the BSC chamber, 3 stage systems.

Requirement	value
Payload Mass	800 kg
Positioning/alignment range	± 1 mm ± 0.25 mrad
Tidal & microseismic actuation range	± 100 μm
Isolation (3 translations)	2×10^{-7} m/√Hz @ 0.2 Hz 1×10^{-11} m/√Hz @ 1 Hz 2×10^{-13} m/√Hz @ 10 Hz 3×10^{-14} m/√Hz @ > 30 Hz
Isolation (3 rotations)	$< 10^{-8}$ rad rms, for $1 < f < 30$ Hz

2.5.2 Design description.

The typical seismic isolation system consists of two or three stages of isolation (Figure 6). The first stage is accomplished with the Hydraulic External Pre-Isolator (HEPI) system, external to the vacuum system. The next one or two stages are referred to as the Internal Seismic Isolation (ISI) system and are contained within the vacuum system. The test mass, beamsplitter and transmission monitor suspensions are supported by inverted optics tables which have two in-vacuum stages, housed in the BSC chambers. All other interferometer elements are supported by upright optics tables connected to one-stage ISI systems, housed in smaller (HAM) vacuum chambers.

The in-vacuum payload is supported by a structure that penetrates the vacuum chamber at four locations, through welded bellows. Each of these four points is supported by a HEPI assembly; each HEPI system supports a total isolated mass of 6400 kg. HEPI employs custom designed, laminar flow, quiet hydraulic actuators (8 per vacuum chamber) in a low frequency (0.1—10 Hz), 6 degree-of-freedom active isolation and alignment system. The actuators employ servo-valves in a hydraulic Wheatstone bridge configuration to control deflection of a diaphragm by differential pressure. For sensors, HEPI uses a blend of geophones and inductive position sensors. In addition, a ground seismometer provides a signal for feed-forward correction.

The ISI[7] consists of three stages (each a stiff mechanical structure) that are suspended and sprung in sequence: stage 0 is the support structure connected to the HEPI frame; stage 1 is suspended and sprung from stage 0; stage 2 is suspended and sprung from stage 1. The stage 2 structure includes the optics table upon which payload elements, such as the suspensions, are attached. Each suspended stage is supported at 3 points by a rod with flexural pivot ends, which are in turn supported by cantilevered blade springs. The springs provide vertical isolation and the flexure rods provide horizontal isolation. They are both made of high strength maraging steel in order to reduce noise resulting from

discrete dislocation movement events associated with creep under load. The springs and flexures allow control in all 6 rigid body degrees-of-freedom of each stage, through the use of electromagnetic force actuation between the stages. Passive isolation from base (stage 0) motion is achieved at frequencies above the rigid body frequencies of these stages.

Stage 1 of the ISI is instrumented with 6 capacitive position sensors (MicroSense), 3 three-axis seismometers (Nanometric Trillium T240) and 6 geophones (Sercel L4C). Stage 2 is instrumented with 6 capacitive position sensors (MicroSense) and 6 geophones (Geotech GS13). The single-axis sensors are equally divided into horizontal and vertical directions. All of the inertial sensors are sealed in vacuum-tight canisters. The 12 electromagnetic actuators (6 between stages 0-1 and 6 between stages 1-2) are equally split between vertical and horizontal orientations, and are a custom, ultra-high vacuum compatible design.

The capacitive position sensor signals provide positioning capability, and are low-pass filtered in the isolation band. For stage 1 control, the T240 and L4C seismometer signals are blended together to provide very low noise and broadband inertial sensing; they are high-pass filtered to remove sensor noise and other spurious low frequency signals, such as tilt for the horizontal sensors. The T240 signals are also used for feed-forward to the stage 2 controller. Before filtering, the sensors are transformed into a Cartesian basis by matrix multiplication in the multi-input, multi-output digital control system.

2.6 Thermal compensation system

Absorption of the Gaussian-profiled laser beam in the core optics causes a non-uniform temperature increase leading to wavefront aberration. Active compensation of this aberration is provided for the test mass optics by the thermal compensation system (TCS).

2.6.2 Design description. The TCS consists of three major elements (see Figure 7): a radiative ring heater (RH), a CO_2 laser projector (CO2P) and a Hartmann wavefront sensor (HWS). The RH is used to correct surface deformation of the ITM and ETM, and to partially correct the ITM substrate thermal lens. The CO2P is used to compensate residual ITM substrate distortions not corrected by the RH. The HWS is used to measure the test mass thermal aberrations.

The basic intent of the combination of the RH and CO2P is to add heat to form the conjugate aberration to the thermal lens formed by the main beam heating. Whereas the RH power stability is good enough to permit direct actuation on the test mass, the CO2P actuates on the compensation plate to limit the effects of CO_2 laser noise.

The RH assembly is comprised of nichrome heater wire wound around two semi-circular glass rod formers, which are housed within a reflective shield; the inner radius of the assembly is 5 mm larger than the test mass radius.

The CO2P is configured to make static pattern corrections via both central and annular projected heating patterns. These two patterns are created using masks that are inserted into the beam using flipper mirrors. The power is adjusted with a polarizer and rotatable ½-waveplate; power fluctuations are stabilized using an AOM. The CO2P is designed to deliver at least 15W to the compensation plate.

The HWS is used to measure the thermal distortions, both before and after compensation. The HWS can measure thermal wavefront distortions with a sensitivity of < 1.4 nm and a spatial resolution of ≤1 cm, both over a 200 mm diameter at the ITM. In the vertex, the HWS uses super-luminescent LEDs (SLED) for probe beams. Independent probe beam

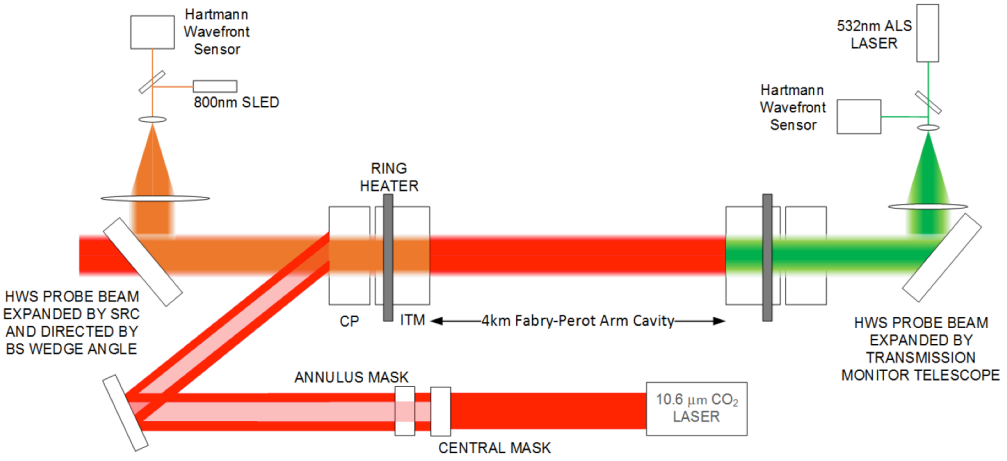

Figure 7 Schematic layout of the Thermal Compensation System for the X-arm. A similar configuration is implemented on the Y-arm, with the SLED probe beam instead transmitting through the BS. Each of the masks can be independently flipped in or out of the beam path.

paths for the X and Y-arms of the Michelson are achieved through choice of SLED wavelength, given the spectral properties of the beam splitter coating: 800 nm is used for the X-arm and 833 nm for the Y-arm (5 mW for both). Both probe beams make use of the beam expansion telescope integral to the signal recycling cavity (SR2 & SR3) to achieve a large profile at the BS, CP and ITM. The HWS for the ETM uses the ALS green laser beam as a probe.

2.7 Scattered light control

The basic design approach for stray light control[8] is to (a) capture all first-order ghost beams in beam dumps, (b) baffle all views of the vacuum envelope (which is not isolated from ground motion), (c) provide baffles and apertures with low light scattering surface properties (low bidirectional reflectance distribution function (BRDF) surfaces), (d) provide baffle geometries which trap specular reflections into multiple reflections, (e) provide surfaces with some amount of absorption, and (f) vibration isolate the baffles.

Surface treatments are restricted due to the need for ultra-high vacuum compatibility. The larger baffles and apertures are oxidized, polished stainless steel surfaces. The depth of the oxidized layer must be carefully controlled to maintain a well-bonded oxide layer and prevent a frangible layer. Smaller baffles and beam dumps are made of black glass. High power, in-vacuum, beam dumps are comprised of polished, chemical vapour deposited silicon carbide.

2.8 Global sensing and control

Using primarily interferometrically generated error signals, active feedback is used to keep the interferometer at the proper operating point. This entails keeping the four interferometer cavities on resonance (two arm cavities, power- and signal-recycling cavity), and the Michelson at the dark fringe (or at a controlled offset from there). In addition, global controls are required to keep the whole interferometer at the proper angular alignment.

2.8.1 Length sensing and control.

Two sets of RF modulation sidebands are applied to the input laser field: one at 9 MHz and one at 45 MHz. Both pairs of RF sidebands are resonant in the power-recycling cavity, but not in the arm cavities. The Michelson has an asymmetry so that RF sideband

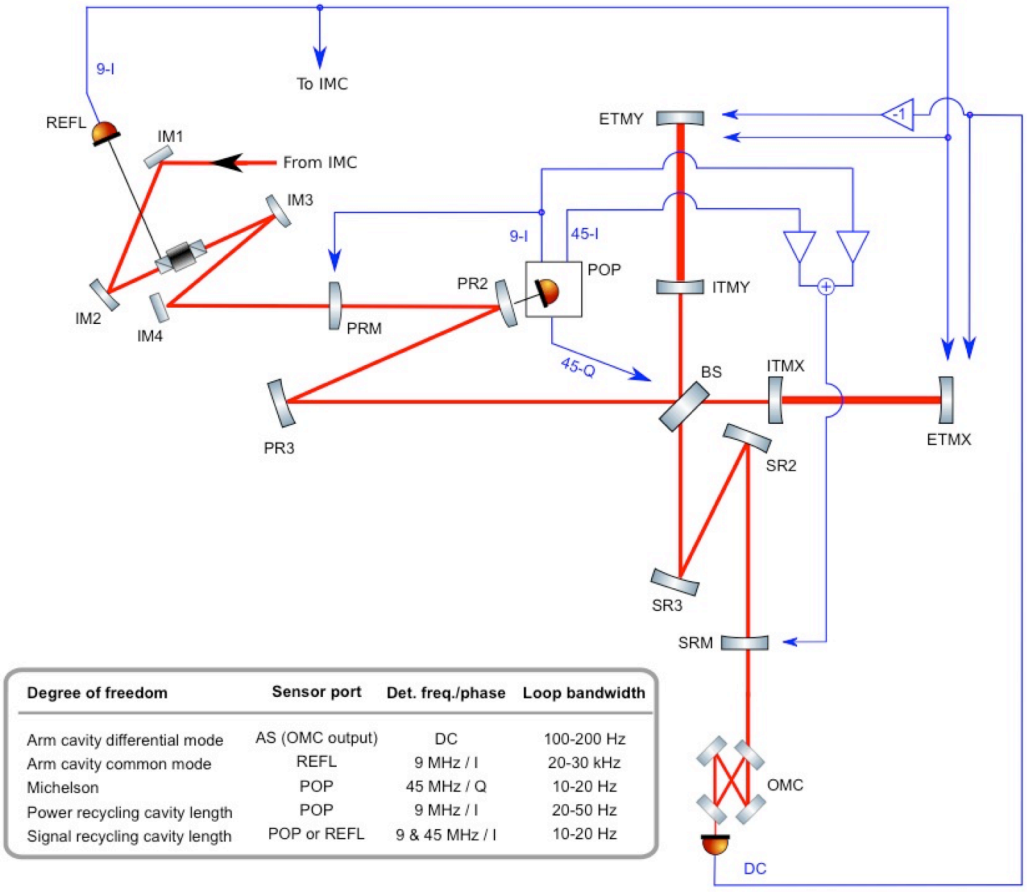

Degree of freedom	Sensor port	Det. freq./phase	Loop bandwidth
Arm cavity differential mode	AS (OMC output)	DC	100-200 Hz
Arm cavity common mode	REFL	9 MHz / I	20-30 kHz
Michelson	POP	45 MHz / Q	10-20 Hz
Power recycling cavity length	POP	9 MHz / I	20-50 Hz
Signal recycling cavity length	POP or REFL	9 & 45 MHz / I	10-20 Hz

Figure 8 Length sensing and control scheme for Advanced LIGO. Though not shown, the Michelson signal is also fed back to the PRM and SRM, so that the BS actuation affects only the Michelson degree-of-freedom.

power is transmitted to the AS port even when the carrier is at the dark fringe. In this case, we choose the asymmetry to couple the majority of the 45 MHz sideband power into the signal recycling cavity.

Figure 8 summarizes the sensing and control scheme for the length degrees-of-freedom. Except for the DC readout of the gravitational wave channel, the length signals are derived from photodetectors at the REFL and POP ports, by demodulating their outputs at one or more of the RF modulation frequencies. The feedback controls are implemented digitally, with a real-time sampling rate of 16,384 samples/sec. The arm common mode loop actuates on the laser frequency so that it follows the highly stable common arm length. The servo includes an analogue feedback path to achieve high bandwidth.

All of the photodetectors used for the length sensing during low-noise operation are located in vacuum chambers, mounted on seismically isolated platforms.

2.8.2 Alignment sensing and control. The residual angular motion of the arm cavity mirrors must be 1 nrad-rms or less to adequately suppress alignment noise effects[9]. Somewhat less stringent angular stability requirements apply to the other interferometer optics. The same phase modulation-demodulation techniques used for the length sensing are used with quadrant photodiodes to produce an alignment wavefront sensor (WFS). Table 8 provides details of the alignment control scheme.

Table 8. Alignment control scheme for the arm cavity mirror (test masses) and the beamsplitter.

Degree of freedom	Sensor type & port	Detection frequency/phase	Loop unity gain frequency
Arm cavity differential hard mode	WFS AS	45 MHz Q-phase	1-few Hz
Arm cavity common hard mode	WFS REFL	9 MHz I-phase	~1 Hz
Arm cavity differential soft mode	QPD TRX-TRY	DC	~1 Hz
Arm cavity common soft mode	QPD TRX+TRY	DC	~1 Hz
Beamsplitter	WFS AS	36 MHz Q-phase	~0.1 Hz

2.8.3 Output mode cleaner and DC readout.

The output mode cleaner (OMC) is designed to filter out all RF sideband and higher-order spatial mode light at the AS port, so that the main photodetectors receive only light

that carries the gravitational wave signal. The OMC is a bowtie cavity with a moderate finesse (400). The nominal OMC round trip length is 1.13 m.

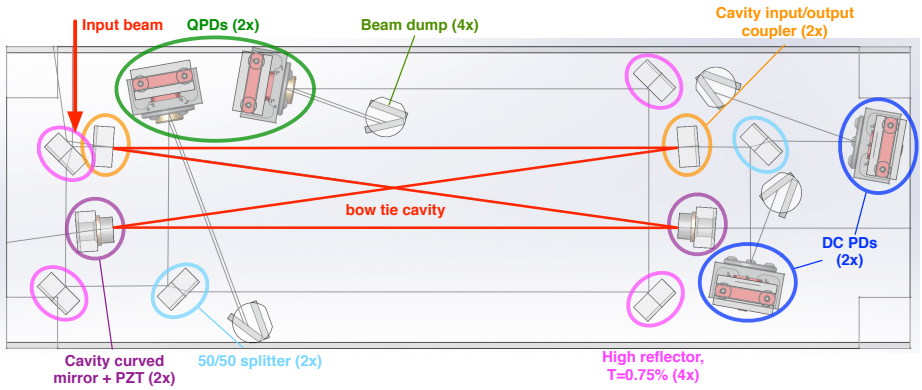

Figure 9 Layout of the OMC on the fused silica breadboard (dimensions 45cm x 15cm x 4.1cm).

As shown in Figure 9, the OMC cavity optics and the output photodiodes are all bonded to a single breadboard of fused silica. The breadboard also includes two QPDs for aid in alignment, and multiple beam dumps for scattered light. Two of the OMC mirrors are mounted on PZT actuators for length control of the cavity. The OMC suspension is mounted in a HAM vacuum chamber on a HAM seismic isolation platform.

The AS port beam is directed into the OMC by three steering optics. These optics provide mode-matching to the OMC, and they are mounted in active single-stage suspensions for vibration isolation and pointing control

2.8.4 Arm length stabilization and lock acquisition. Lock acquisition is the process of bringing the interferometer to its operating point, with all the cavities resonant so that power buildup is at a maximum.

The arm length stabilization system (ALS) locks each arm cavity individually using a laser mounted behind each end test mass. This is shown schematically in Figure 10. The ALS lasers are doubled Nd:YAG lasers, operating at 532 nm to distinguish them from the main laser light; they also have a 1064 nm output which is used to phase (frequency offset) lock them to the main laser light. The test masses have dichroic coatings designed to create a relatively low finesse cavity for 532 nm, with reasonable transmission of 532 nm light to the vertex beamsplitter.

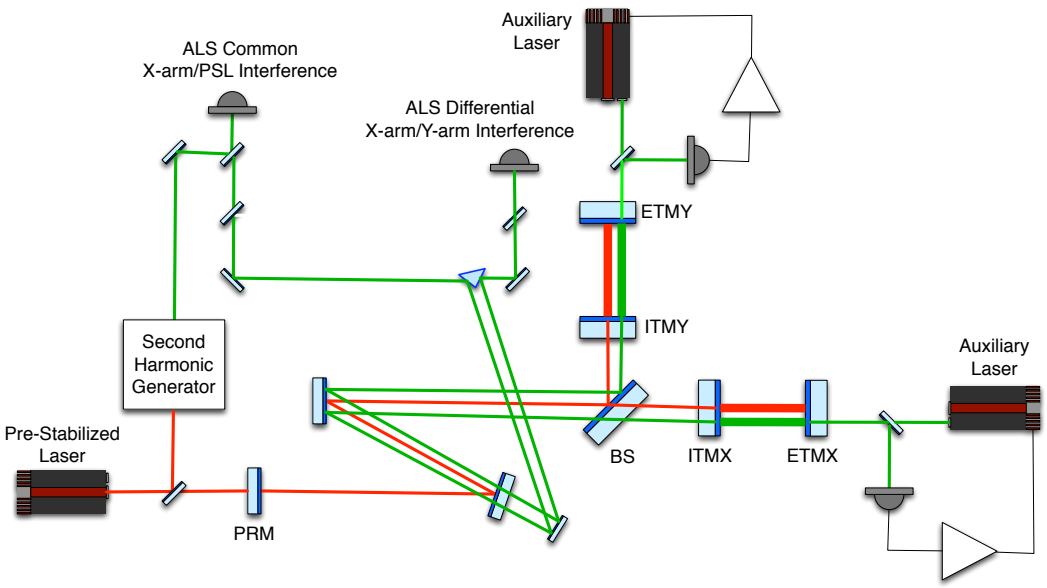

Figure 10 Simplified schematic of the arm length stabilization system.

2.9 Transmission Monitor Suspension

The Transmission Monitoring Suspension:

- Collects 1064 nm light transmitting through the end test mass (ETM) and provides it for Interferometer Sensing and Control
- Mode matches 532 nm light for Arm Length Stabilization
- Provides input for intermittent Hartmann monitoring system
- Transmits any residual 1064 nm radiation to a beam dump

The TMS assembly consists of an optics platform, a suspension for that platform, a beam reducing telescope, and various opto-mechanical and opto-electronic components for beam detection and control.

2.10 Calibration

The photon calibration uses an auxiliary, power-modulated laser to create displacements via photon recoil off the surface of the ETM (Figure 11). Two beams are used, offset symmetrically from the mirror center. The laser power is measured with a temperature stabilized InGaAs photodetector mounted on an integrating sphere, which is calibrated against a NIST-calibrated standard. The lasers are 2 W continuous-wave, 1047nm

Nd:YLF lasers. An AOM enables power modulation, up to a peak-to-peak sinusoidal modulation of 1 W, producing an ETM displacement of 10^{-16} m-rms at 100 Hz.

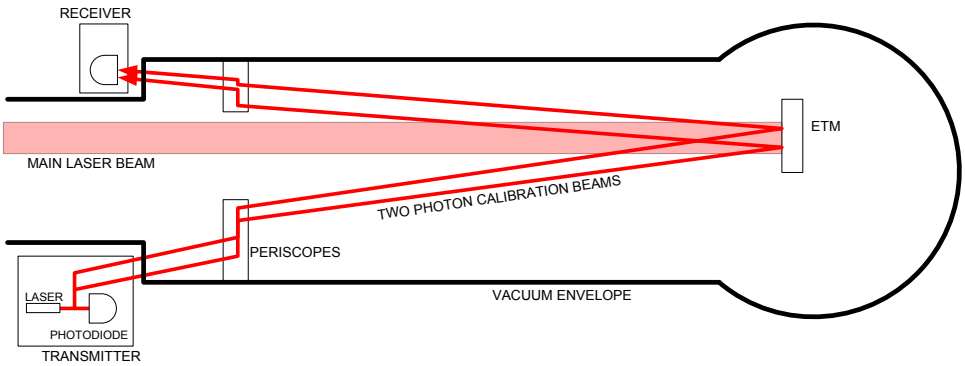

Figure 11 Schematic of the photon calibration system.

2.11 Controls and data acquisition

Many of the subsystems employ real-time digital controls in their functioning; data from other subsystems and channels must be acquired in real-time for archiving and analysis. A custom data acquisition architecture, diagrammed in Figure 12, is implemented to serve these needs. Interferometer sensor and actuator signals flow through custom input-output chassis (IOC). Each IOC houses: a 17 slot PCI Express (PCIe) backplane; a timing module that provides accurate triggering at 65536 Hz and is synchronized with the interferometer timing distribution system; a commercial fibre optic PCIe uplink to a real-time control computer. The PCIe slots are populated specifically for each IOC, but primarily contain commercial multi-channel, simultaneous sampling 16-bit analogue-to-digital and 16 and 18-bit digital-to-analogue converters (ADCs and DACs). Custom anti-alias and anti-image filters interface between the ADCs and DACs and the analogue signals. The IOCs and filters are located in rooms separate from the vacuum chamber areas to mitigate electronic and acoustic interference with sensitive interferometer components.

The real-time control computers are located yet further from the interferometer, in a separate computer room, and are linked via fibre. The computers are commercial, multi-core rack mount units, specially selected for compatibility with real-time operation: there must be no uncontrollable system interrupts, and they must be capable of supporting the required number of PCIe modules.

The system is designed to support servo loop rates of up to 65536 Hz, which requires real-time execution to be precise and repeatable to within a few microseconds, and synchronized across the site.

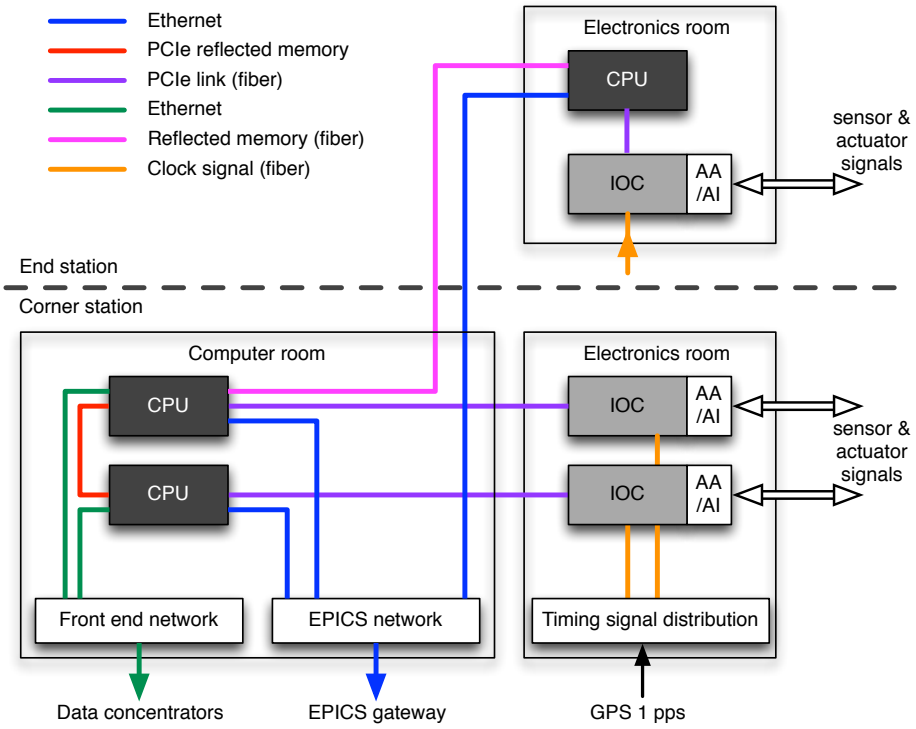

Figure 12 Schematic of the data acquisition architecture.

References

1. Palashov *et al* 2012 *J. Opt. Soc. Am. B* **29** 1784-1792
2. Aston S M *et al* 2012 *Class. Quantum Grav.* **29** 235004
3. Beccaria M *et al* 1998 *Nucl. Instr. and Meth. In Phys. Res. A* **404** 455-469
4. Carbone L *et al* 2012 *Class. Quantum Grav.* **29** 115005
5. Hewitson H, Danzmann K, Grote H, Hild S, Hough J, Luck H, Rowan S, Smith J R, Strain K A and Willke B 2007 *Class. Quantum Grav.* **24** 6379—6391
6. Heptonstall A *et al* 2011 *Rev. Sci. Instrum.* **82** 011301
7. Matichard F *et al* 2014 Advanced LIGO Two-Stage Twelve-Axis Vibration Isolation and Positioning Platform. Part 1: Design and Production Overview. *Precision Eng.* http://dx.doi.org/10.1016/j.precisioneng.2014.09.010, Part 2: Experimental Investigation and Test Results. *Precision Eng.* http://dx.doi.org/10.1016/j.precisioneng.2014.11.010
8. Smith M R 2009 *Proc. 12th Marcel Grossman Meeting on General Relativity, July 2009, UNESCO Headquarters, Paris* ed Damour T, Jantzen R, Ruffini R (Singapore: World Scientific) 1735
9. Mueller G 2005 *Optics Express* **13** 7118